

Angular momentum transfer in multinucleon transfer channels of $^{18}\text{O} + ^{237}\text{Np}$ S. Tanaka ^{1,2}, K. Hirose,² K. Nishio ², K. R. Kean ^{3,2}, H. Makii ², R. Orlandi ², K. Tsukada,² and Y. Aritomo ¹¹*Graduate School of Science and Engineering, Kindai University, Higashi-Osaka 577-8502, Japan*²*Advanced Science Research Center, Japan Atomic Energy Agency, Tokai, Ibaraki 319-1195, Japan*³*Laboratory for Advanced Nuclear Energy, Institute for Innovative Research, and Department of Trans-disciplinary Science and Engineering, School of Environment and Society, Tokyo Institute of Technology, Ookayama, Meguro-ku, Tokyo 152-8550, Japan*

(Received 25 September 2021; accepted 10 December 2021; published 15 February 2022)

The angular momentum of a primary excited compound nucleus produced in multinucleon transfer reaction is an important quantity to evaluate cross sections to synthesize neutron-rich heavy-element nuclei as well as for surrogate reaction studies. The mechanism is, however, not enough understood due to the lack of detailed experimental data. In the present study, we determined the angular momentum of primary excited nuclei, $^{237,238,239}\text{Np}$, $^{238,239,240}\text{Pu}$, and $^{239,240,241}\text{Am}$, produced in the multinucleon transfer channels of the $^{18}\text{O} + ^{237}\text{Np}$ reaction. With this aim, angular distributions of fission fragments with respect to the axis perpendicular to the reaction plane were measured for each compound nucleus. The distributions show an anisotropy exhibiting an enhanced yield on the reaction plane. They are well reproduced by a saddle-point model, from which the average angular momentum is derived in the model framework. The angular momentum increases with the compound-nucleus mass, thus the number of nucleons exchanged, but shows a saturating trend toward heavier compound nuclei. These results are the first ones to point to the dependence of the angular momentum on the transfer channels.

DOI: [10.1103/PhysRevC.105.L021602](https://doi.org/10.1103/PhysRevC.105.L021602)

Recently, multinucleon transfer (MNT) reactions in heavy-ion collisions have attracted considerable interest in the nuclear physics community. These reactions have the potential to produce neutron-rich nuclei in the superheavy element (SHE) region that cannot be approached with fusion reactions using available ion beams and targets [1–7]. In MNT reactions, there is a larger probability for the transfer of neutrons than of protons from the projectile to the target, resulting in the production of neutron-rich compound nuclei. Accordingly, heavy-element nuclei produced as evaporation residues can also be neutron-rich. In contrast with the production of elements lighter than lead [8–10], in the region of actinides, fission becomes a competing decay channel, thus reducing significantly their production cross section. As the survival probability sensitively decreases with excitation energy and angular momentum of the primary compound nucleus, their population mechanism should be understood in order to accurately predict the cross sections of neutron-rich superheavy nuclei. The excitation-energy distribution of the primary products in the MNT process can be obtained from the measurement of the kinetic energy of the ejectile nuclei [10–16].

In general, the angular momentum can be determined by observing the angular correlation of decay products with respect to a space-fixed axis. The detection of fission-fragments is one of the possible experimental approaches. In the statistical transition state model (TSM) [17], by defining an axis of angular momentum, which mostly originates from the rotational motion of nucleus, fission fragments are

emitted preferentially in the direction perpendicular to the axis, i.e., on the reaction plane defined by the direction of the beam and the recoil. This behavior is amplified when larger angular momentum is stored in the nucleus, causing larger fission-fragment angular anisotropy. The TSM adequately describes the measured angular distributions in the fission of compound nuclei produced by fusion [18–21]. In the framework of the TSM, angular-momentum transfer was studied in the deep-inelastic scattering of $^{86}\text{Kr} + ^{209}\text{Bi}$ [22,23] by adopting a formula derived in Refs. [24,25]. In their study of $^{86}\text{Kr} + ^{209}\text{Bi}$, the angular momentum of target-like products is found to change with the total excitation energy of the exit channel, but the dependence of the angular momentum on the number of transferred protons is not so evident due to large errors. Fission-fragment angular anisotropies were reported in the study of the MNT reaction of $^{16}\text{O} + ^{232}\text{Th}$ [25], in which different transfer channels were separated using silicon ΔE - E telescope detectors. The variation of angular momentum with respect to the mass of the transferred nucleons, however, is poorly understood due to insufficient data points in the angular distributions. In the present study, we report the measurement of fission-fragment angular distributions for each MNT channel of the $^{18}\text{O} + ^{237}\text{Np}$ reaction, from which the average angular momentum for each transfer channel was quantified using the TSM. This measurement is also important for the study of surrogate reactions [26,27]. In this method, single- and multinucleon transfer reactions are used to evaluate neutron-capture and/or fission cross sections by populating the same compound nucleus of interest and measuring γ -ray

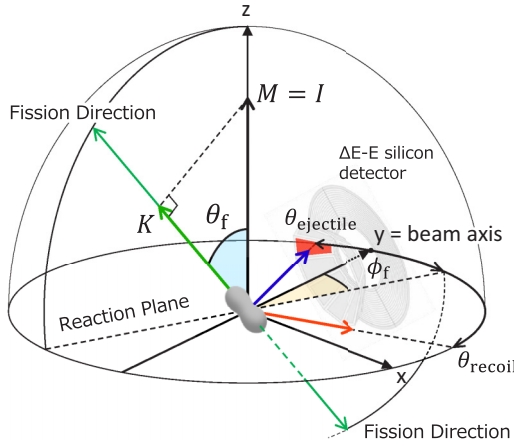


FIG. 1. Geometry of the experiment.

transition or fission probability. As the Weisskopf-Ewing limit is not applicable in general [26], the decay probability, thus the derived cross sections, sensitively depends on the spins of the compound nucleus. Using experimental data to evaluate the spins for each transfer channel is also required.

The angular-distribution data in this study were obtained from the MNT experiment of $^{18}\text{O} + ^{237}\text{Np}$, already reported in Ref. [16] to discuss fission-fragment mass distributions. The experimental method is described in Refs. [14–16], thus only the essential information is given here. The experiment was performed using a 162.0-MeV ^{18}O beam supplied by the JAEA tandem accelerator in Tokai, Japan. A schematic diagram describing how the fragments angular distribution is measured is shown in Fig. 1. The setup consists of an array of ΔE - E silicon telescope to detect ejectiles and four multiwire proportional counters (MWPCs, 200 mm \times 200 mm each), to detect fission fragments (FFs). The MWPCs were placed at $\pm 50^\circ$ and $\pm 130^\circ$ with respect to the beam direction. Specific particle-transfer channels were determined by identifying the ejectiles using the ΔE - E telescope placed at a forward angle, which cover the scattering angle θ_{ejectile} from 16.7° to 31.0° relative to the beam direction. Thus the compound nucleus is identified on a event-by-event basis, assuming the binary reaction. An ejectile passes through one of the 12 ΔE detectors ($75 \mu\text{m}$ thick) to give the energy-loss ΔE and is stopped in the 16-strip annular E detector ($300 \mu\text{m}$ thick) to give residual energy E_{res} . The ejectile kinetic energy, $E_{\text{ejectile}} = \Delta E + E_{\text{res}}$, is used to deduce the excitation energy of the exit channel. Figure 2 shows the projection of the ΔE - E plot along the particle-identification curves for events in coincidence with both fragments and corresponding to an excitation-energy range of the compound nuclei between 10 and 20 MeV. A good separation between different isotopes, thus different compound nuclides, is achieved. Contamination from the adjacent nuclei in the gating procedure is as small as 4.6% on average. This probability was estimated from the overlapped area of the Gaussian distributions that represent the produced isotopes, shown by the blue curves in Fig. 2.

The reaction plane is defined by the ΔE -detector number. The scattering angle θ_{ejectile} and the ejectile energy E_{ejectile} define the recoil direction θ_{recoil} . The emission angle of each

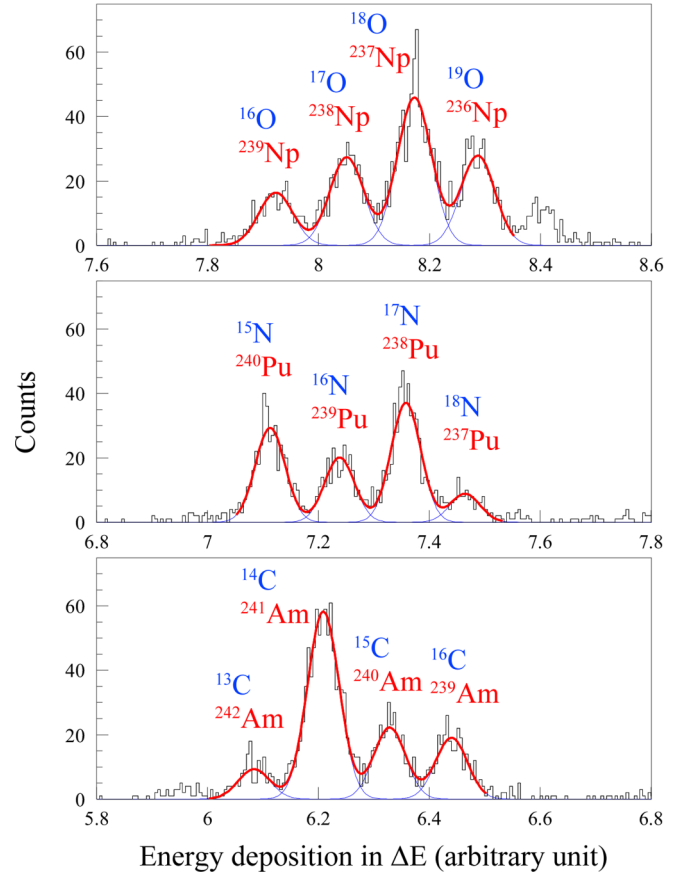


FIG. 2. Identification of ejectile nuclei (labeled in blue) by the silicon ΔE - E telescope (data collected in $E^* = 10$ – 20 MeV) in the study of the $^{18}\text{O} + ^{237}\text{Np}$ reaction. The corresponding fissioning compound nuclei are shown in red. The light blue curves show the results of the multi-Gaussian fitting, and the red curve is the sum of them.

fission fragment, θ_f , is defined by the angle relative to the z axis. In the data analysis, we used those events in which two fragments are detected in coincidence. We assumed that the angular momentum is fully aligned to the z direction. In this case, there is no in-plane angular anisotropy. We thus show the out-of-plane angular distribution, $W(\theta_f)$, which does not change with respect to the azimuthal angle ϕ_f , see Fig. 1. The out-of-plane angular distribution, with respect to the z axis for the nine compound nuclides ($^{237,238,239}\text{Np}$, $^{238,239,240}\text{Pu}$, and $^{239,240,241}\text{Am}$) are shown in Fig. 3. The distributions are obtained using fission events entering in the excitation-energy range of $E^* = 10$ – 20 MeV. In this region, the probability of second- and higher-chance fission is small [15,28]. In Fig. 3, the events in the range of $\theta_f = 0^\circ$ – 15° and $\theta_f = 165^\circ$ – 180° were not determined due to the large uncertainty in estimating the detection efficiency for fission fragments. Each distribution shows a pronounced peak at $\theta_f = 90^\circ$. It indicates a strong angular anisotropy with an enhanced yield on the reaction plane. It is found that the angular anisotropy of compound nuclei produced by exchanging nucleons is far larger than the inelastic channel ($^{237}\text{Np}^*$). The large anisotropy is a direct

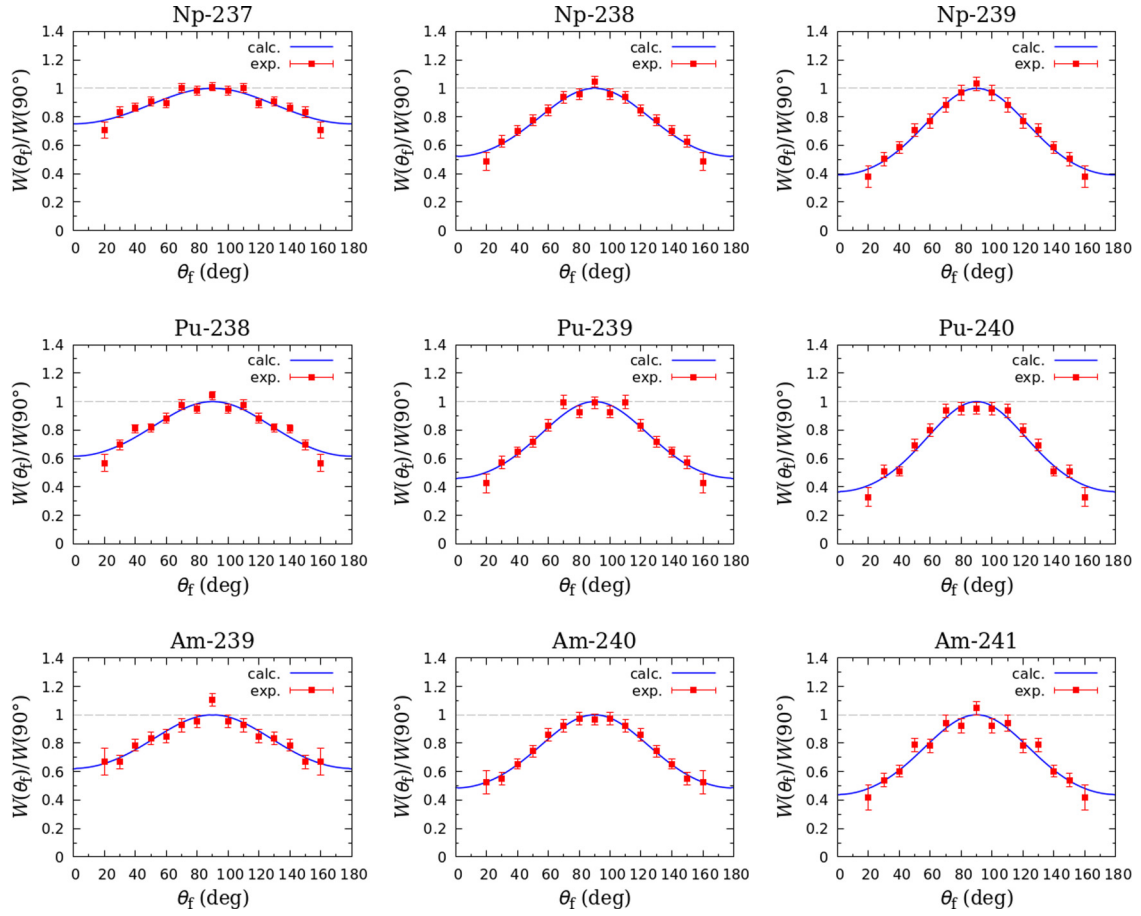


FIG. 3. Experimental angular distributions of fission fragments ($^{237,238,239}\text{Np}$, $^{238,239,240}\text{Pu}$, and $^{239,240,241}\text{Am}$) from the MNT channels of $^{18}\text{O} + ^{237}\text{Np}$ ($E_{\text{lab}} = 162$ MeV) (red points). Results of the fits to Eq. (2) are shown by the solid line. The horizontal dash lines show $W(\theta_f)/W(90^\circ) = 1$.

indication of sizable angular-momentum transfer carried by the transferred nucleons.

In the TSM, the direction of the fission fragments is determined by the K quantum states at the saddle point, i.e., the projection of the spin I on the symmetry axis of the nucleus (fission direction) [29]. Thus the measured fission-fragment angular distribution is regulated by the distribution of K quantum states. The angular distribution of fission fragments with respect to the z axis and from a nucleus having quantum numbers I , M , and K is given by

$$W_{MK}^I(\theta_f) = \frac{1}{2}(2I+1)|d_{MK}^I(\theta_f)|^2, \quad (1)$$

where M is the projection of I on the z axis, and $d_{MK}^I(\theta_f)$ is the rotational wave function. Assuming that the angular momentum aligns on the z axis, $M = \pm I$ holds. This results in the expression [24,30]

$$W(\theta_f) = \sum_{I=0}^{\infty} F(I) \sum_{K=-I}^{+I} \left\{ \frac{(2I+1)|d_{\pm IK}^I(\theta_f)|^2 e^{-\frac{K^2}{2K_0^2}}}{\sum_{K=-I}^{+I} e^{-\frac{K^2}{2K_0^2}}} \right\}, \quad (2)$$

where $F(I)$ is the spin distribution of the compound nucleus, given below. Here the distribution of the K quantum number is assumed to be a Gaussian with the square of the standard

deviation, K_0^2 , defined by

$$K_0^2 = I_{\text{eff}}T/\hbar^2. \quad (3)$$

Here, I_{eff} is the effective moment of inertia and $T = (E_{\text{saddle}}^*/a)^{1/2}$ is the saddle-point nuclear temperature. The level density of a compound nucleus of mass A_{cn} is taken to be $a = A_{\text{cn}}/10$ MeV $^{-1}$. The excitation energy at the saddle point E_{saddle}^* is given by $E_{\text{saddle}}^* = E_{\text{c.m.}} + Q - B_f - E_{\text{rot}}$, where Q is the Q value for the formation of the compound nucleus. The spin-dependent fission barrier B_f , ground-state rotational energy E_{rot} , and effective moment of inertia I_{eff} are calculated by using the model in Ref. [31].

For the $F(I)$ distribution, we assume a Gaussian-like shape with the average value I_0 and the standard deviation $\sigma = \sqrt{I_0}$. The results of the fit with Eq. (2) by changing I_0 are shown by the solid curves in Fig. 3. The results reproduce the data reasonably well. The obtained I_0 values and angular anisotropies defined by $W(90^\circ)/W(0^\circ)$ are given in Table I. In addition, the dependence of I_0 on A_{cn} is shown in Fig. 4. It is seen that the average angular momentum increases with the number of transferred nucleons, but tends to saturate at $15\hbar$. The present results are the first to clearly show the relation between the transferred nucleon numbers and the angular momentum.

TABLE I. Fissioning nucleus and the number of transferred nucleons from projectile to target, K_0 values, fission fragment angular anisotropy $W(90^\circ)/W(0^\circ)$, mean transferred angular momentum I_0 , and calculated orbital angular momentum l_{gr} (with incident particle) are tabulated.

Channel	K_0	$W(90^\circ)/W(0^\circ)$	I_0 (\hbar)	l_{gr} (\hbar)
^{237}Np ($0p0n$)	9.57	1.33 ± 0.15	7.1 ± 1.5	
^{238}Np ($0p1n$)	9.59	1.92 ± 0.23	11.0 ± 1.1	
^{239}Np ($0p2n$)	9.61	2.56 ± 0.31	13.4 ± 1.0	
^{238}Pu ($1p0n$)	10.10	1.62 ± 0.26	9.9 ± 1.8	5 (p)
^{239}Pu ($1p1n$)	10.11	2.17 ± 0.63	12.7 ± 1.7	11 (d)
^{240}Pu ($1p2n$)	10.13	2.72 ± 0.63	14.6 ± 1.8	19 (t)
^{239}Am ($2p0n$)	10.64	1.60 ± 0.28	10.3 ± 2.0	
^{240}Am ($2p1n$)	10.65	2.06 ± 0.17	12.9 ± 0.8	13 (^3He)
^{241}Am ($2p2n$)	10.64	2.27 ± 0.49	13.8 ± 2.0	21 (^4He)

The magnitude of the angular momentum is consistent with the one implied from the measured fission-fragment mass distributions of the compound nuclei from the MNT reaction [16]. In this work, the measured FFMDs are compared with the Langevin calculation which takes into account multichance fission. The probability for each fission chance depends sensitively on the spins introduced in the compound nucleus and thus alters the shape of FFMDs at high excitation energies. The measured FFMDs are explained in the calculation when the spins are less than $20\hbar$.

It is argued that the angular distribution is primarily determined by the average value of the spins, I_0 , and is not very sensitive to how the spins are distributed around I_0 [22,24,25,32]. This was confirmed by using different types of $F(I)$, still keeping the same I_0 value. We examined two additional types of $F(I)$. One is the δ -function $F(I) = \delta(I - I_0)$, the other is the $F(I) = (2I + 1)$ ending at the maximum I_{max} . As a result, the best fit I_0 value using three $F(I)$ functions all agree within $1\hbar$.

To interpret the obtained angular momentum quantitatively, we made a simple classical calculation assuming that the angular momentum is equal to the orbital angular momentum l_{gr} that a bulk of several nucleons (cluster), contained in the incident nucleus and transferred to the target nucleus, have at the grazing collision. Here, the cluster should have the same velocity as ^{18}O , and the coupled-channel calculation using CCFUL [33] is adopted by treating $^{1,2,3}\text{H}$ and $^{3,4}\text{He}$ as clusters. The results are shown in Table I and Fig. 4. It is found that l_{gr} increases with A_{cn} more rapidly than the experimental data. For a fixed number of transferred nucleons, the calculation shows a sizable difference between neutron and proton transfer (see the data points for t and ^3He). This is in contrast with the experimental data. Still, overall, the magnitude of the

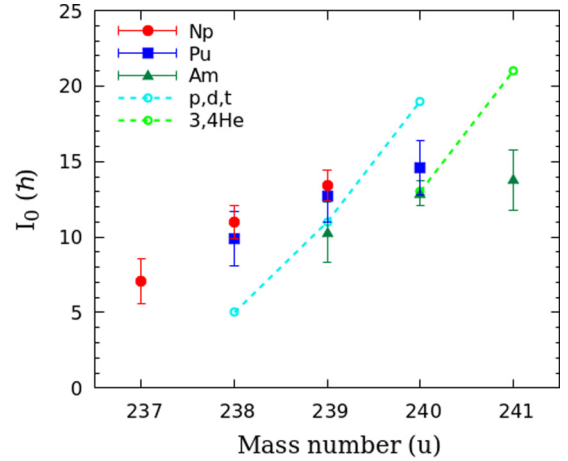


FIG. 4. Average angular momenta obtained from the fission-fragment angular distribution are shown by the different symbols for different atomic number of compound nuclei. The dashed curve is the calculated angular momentum (see text for detail) for impinging clusters of $^{1,2,3}\text{H}$ (light blue dashed-curve) and $^{3,4}\text{He}$ (light green dashed-line) at the grazing collision.

calculated angular momentum agrees within $\approx 5\hbar$.

In this experiment, it is assumed that the fission fragments are emitted isotropically in the reaction plane, because the present setup has a relatively large uncertainty in evaluating the detection efficiency as a function of ϕ_f . In general, however, anisotropy also occurs in-plane [22,23]. This indicates that the rotational axis is not fully polarized to the z axis ($I \neq M$) but has a component on the x and/or y axis. In this case, the angular momentum can have a larger value than that in Table I. Referring to the spin orientation discussed in Ref. [23], the average angular momentum could increase by approximately $3\hbar$.

We determined the angular-momentum transferred to the compound nucleus by measuring the fission-fragment angular distribution with respect to the axis perpendicular to the reaction plane. The MNT transfer channel, thus the fissioning compound nucleus, is clearly identified by using the ΔE - E telescope. The angular momentum increases with the compound-nucleus mass, thus with the number of nucleons exchanged, but exhibits a saturating trend at $15\hbar$. These results are the first to clearly show the dependence of the angular momentum on the transfer channels. We plan to further investigate the angular-momentum transfer using also other heavy-ion collisions.

We thank the crew of the tandem accelerator facility for supplying the high-quality stable beam.

- [1] M. Schädel, J. V. Kratz, H. Ahrens, W. Brüche, G. Franz, H. Gäggeler, I. Warnecke, G. Wirth, G. Herrmann, N. Trautmann, and M. Weis, *Phys. Rev. Lett.* **41**, 469 (1978).
 [2] M. Schädel, W. Brüche, H. Gäggeler, J. V. Kratz, K. Stümmerer, G. Wirth, G. Herrmann, R. Stakemann, G. Tittel, N. Trautmann, J. M. Nitschke, E. K. Hulet, R. W. Loughheed,

R. L. Hahn, and R. L. Ferguson, *Phys. Rev. Lett.* **48**, 852 (1982).

[3] V. I. Zagrebaev and W. Greiner, *Phys. Rev. C* **83**, 044618 (2011).

[4] V. V. Saiko and A. V. Karpov, *Phys. Rev. C* **99**, 014613 (2019).

[5] K. Sekizawa and K. Yabana, *Phys. Rev. C* **93**, 054616 (2016).

- [6] H. M. Devaraja, S. Heinz, D. Ackermann, T. Göbel, F. P. Heßberger, S. Hofmann, J. Maurer, G. Münzenberg, A. G. Popeko, and A. V. Yeremin, *Eur. Phys. J. A* **56**, 224 (2020).
- [7] G. G. Adamian, N. V. Antonenko, A. Diaz-Torres, and S. Heinz, *Eur. Phys. J. A* **56**, 47 (2020).
- [8] J. S. Barrett, W. Loveland, R. Yanez, S. Zhu, A. D. Ayangeakaa, M. P. Carpenter, J. P. Greene, R. V. F. Janssens, T. Lauritsen, E. A. McCutchan, A. A. Sonzogni, C. J. Chiara, J. L. Harker, and W. B. Walters, *Phys. Rev. C* **91**, 064615 (2015).
- [9] Y. X. Watanabe, Y. H. Kim, S. C. Jeong, Y. Hirayama, N. Imai, H. Ishiyama, H. S. Jung, H. Miyatake, S. Choi, J. S. Song, E. Clement, G. de France, A. Navin, M. Rejmund, C. Schmitt, G. Pollarolo, L. Corradi, E. Fioretto, D. Montanari, M. Niikura *et al.*, *Phys. Rev. Lett.* **115**, 172503 (2015).
- [10] T. Mijatović, S. Szilner, L. Corradi, D. Montanari, G. Pollarolo, E. Fioretto, A. Gadea, A. Goasduff, D. J. Malenica, N. Mărginean, M. Milin, G. Montagnoli, F. Scarlassara, N. Soić, A. M. Stefanini, C. A. Ur, and J. J. Valiente-Dobón, *Phys. Rev. C* **94**, 064616 (2016).
- [11] L. Corradi, A. M. Stefanini, C. J. Lin, S. Beghini, G. Montagnoli, F. Scarlassara, G. Pollarolo, and A. Winther, *Phys. Rev. C* **59**, 261 (1999).
- [12] C. Rodríguez-Tajes, F. Farget, X. Derkx, M. Caamaño, O. Delaune, K.-H. Schmidt, E. Clément, A. Dijon, A. Heinz, T. Roger, L. Audouin, J. Benlliure, E. Casarejos, D. Cortina, D. Doré, B. Fernández-Domínguez, B. Jacquot, B. Jurado, A. Navin, C. Paradela *et al.*, *Phys. Rev. C* **89**, 024614 (2014).
- [13] Sonika, B. J. Roy, A. Parmar, U. K. Pal, H. Kumawat, V. Jha, S. K. Pandit, V. V. Parkar, K. Ramachandran, K. Mahata, A. Pal, S. Santra, A. K. Mohanty, and K. Sekizawa, *Phys. Rev. C* **92**, 024603 (2015).
- [14] R. Léguillon, K. Nishio, K. Hirose, H. Makii, I. Nishinaka, R. Orlandi, K. Tsukada, J. Smallcombe, S. Chiba, Y. Aritomo, T. Ohtsuki, R. Tatsuzawa, N. Takaki, N. Tamura, S. Goto, I. Tsekhanovich, C. M. Petrache, and A. N. Andreyev, *Phys. Lett. B* **761**, 125 (2016).
- [15] K. Hirose, K. Nishio, S. Tanaka, R. Léguillon, H. Makii, I. Nishinaka, R. Orlandi, K. Tsukada, J. Smallcombe, M. J. Vermeulen, S. Chiba, Y. Aritomo, T. Ohtsuki, K. Nakano, S. Araki, Y. Watanabe, R. Tatsuzawa, N. Takaki, N. Tamura, S. Goto *et al.*, *Phys. Rev. Lett.* **119**, 222501 (2017).
- [16] M. J. Vermeulen, K. Nishio, K. Hirose, K. R. Kean, H. Makii, R. Orlandi, K. Tsukada, I. Tsekhanovich, A. N. Andreyev, S. Ishizaki, M. Okubayashi, S. Tanaka, and Y. Aritomo, *Phys. Rev. C* **102**, 054610 (2020).
- [17] R. Vandenbosch and J. R. Huizenga, *Nuclear Fission* (Academic Press, New York, 1973).
- [18] B. B. Back, *Phys. Rev. C* **31**, 2104 (1985).
- [19] B. B. Back, R. R. Betts, J. E. Gindler, B. D. Wilkins, S. Saini, M. B. Tsang, C. K. Gelbke, W. G. Lynch, M. A. McMahan, and P. A. Baisden, *Phys. Rev. C* **32**, 195 (1985).
- [20] D. J. Hinde, M. Dasgupta, J. R. Leigh, J. C. Mein, C. R. Morton, J. O. Newton, and H. Timmers, *Phys. Rev. C* **53**, 1290 (1996).
- [21] D. J. Hinde, W. Pan, A. C. Berriman, R. D. Butt, M. Dasgupta, C. R. Morton, and J. O. Newton, *Phys. Rev. C* **62**, 024615 (2000).
- [22] P. Dyer, R. J. Puigh, R. Vandenbosch, T. D. Thomas, and M. S. Zisman, *Phys. Rev. Lett.* **39**, 392 (1977).
- [23] P. Dyer, R. J. Puigh, R. Vandenbosch, T. D. Thomas, M. S. Zisman, and L. Nunnelley, *Nucl. Phys. A* **322**, 205 (1979).
- [24] B. B. Back and S. Bjornholm, *Nucl. Phys. A* **302**, 343 (1978).
- [25] F. Videbaek, S. G. Steadman, G. G. Batrouni, and J. Karp, *Phys. Rev. C* **35**, 2333 (1987).
- [26] J. E. Escher, J. T. Burke, F. S. Dietrich, N. D. Scielzo, I. J. Thompson, and W. Younes, *Rev. Mod. Phys.* **84**, 353 (2012).
- [27] R. Pérez Sánchez, B. Jurado, V. Méot, O. Roig, M. Dupuis, O. Bouland, D. Denis-Petit, P. Marini, L. Mathieu, I. Tsekhanovich, M. Aïche, L. Audouin, C. Cannes, S. Czajkowski, S. Delpech, A. Görgen, M. Guttormsen, A. Henriques, G. Kessedjian, K. Nishio, D. Ramos *et al.*, *Phys. Rev. Lett.* **125**, 122502 (2020).
- [28] S. Tanaka, Y. Aritomo, Y. Miyamoto, K. Hirose, and K. Nishio, *Phys. Rev. C* **100**, 064605 (2019).
- [29] E. Wigner, *Trans. Faraday Soc.* **34**, 29 (1938).
- [30] J. R. Huizenga, A. N. Behkami, and L. G. Moretto, *Phys. Rev.* **177**, 1826 (1969).
- [31] A. J. Sierk, *Phys. Rev. C* **33**, 2039 (1986).
- [32] J. P. Lestone, J. R. Leigh, J. O. Newton, and J. X. Wei, *Nucl. Phys. A* **509**, 178 (1990).
- [33] K. Hagino, N. Rowley, and A. T. Kruppa, *Comput. Phys. Commun.* **123**, 143 (1999).